World Academy of Science, Engineering and Technology
International Journal of Mechanical and Mechatronics Engineering
Vol:17, No:10, 2023

A Simulation Study of Direct Injection Compressed Natural Gas Spark Ignition Engine Performance Utilizing Turbulent Jet Ignition with Controlled Air Charge

Siyamak Ziyaei, Siti Khalijah Mazlan, Petros Lappas

Abstract—Compressed natural gas (CNG) is primarily composed of methane (CH_4), and has a lower carbon to hydrogen ratio than other hydrocarbon fuels such as gasoline (C_8H_{18}) and diesel ($C_{12}H_{23}$). Consequently, it has the potential to reduce CO_2 emissions compared to conventional fuels. Although Natural Gas (NG) has environmental advantages compared to other hydrocarbon fuels, its main component, CH_4, burns at a slower rate compared to the conventional fuels. A higher pressure and leaner cylinder environment will unravel the slow burn characteristic of CH_4. Lean combustion and high compression ratios are well-known methods for increasing the efficiency of internal combustion engines. In order to achieve successful a CNG lean combustion in Spark Ignition (SI) engines, a strong ignition system is essential to avoid engine misfires, especially in ultra-lean conditions. Turbulent Jet Ignition (TJI) is an ignition system that employs a pre-combustion chamber to ignite the lean fuel mixture in the main combustion chamber using a fraction of the total fuel per cycle. TJI enables ultra-lean combustion by providing distributed ignition sites through orifices. The fast burn rate provided by TJI enables the ordinary SI engine to be comparable to other combustion systems such as Homogeneous Charge Compression Ignition (HCCI) or Controlled Auto-Ignition (CAI) in terms of thermal efficiency, through the increased levels of dilution without the need of sophisticated control systems. Due to the physical geometry of TJI, which contains small orifices that connect the pre-chamber to the main chamber, providing the right mixture of fuel and air has been identified as a key challenge due to the insufficient amount of air that is pushed into the pre-chamber during each compression stroke. There is also the problem of scavenging which contributed to the factors that reduces the TJI performance. Combustion residual gases such as CO_2, CO and NO_x from the previous combustion cycle dilute the pre-chamber fuel-air mixture preventing rapid combustion in the pre-chamber. An air-controlled active TJI is presented in this paper in order to address these issues. By supplying air into the pre-chamber at a sufficient pressure, residual gases are exhausted, and the air-fuel ratio is controlled within the pre-chamber, thereby improving the quality of the combustion. An investigation of the 3D combustion characteristics of a CNG-fueled SI engine using a direct injection fuelling strategy employing an air channel in the prechamber is presented in this paper. Experiments and simulations were performed at the Worldwide Mapping Point (WWMP) at 1500 revolutions per minute (rpm), 3.3 bar Indicated Mean Effective Pressure (IMEP), using only conventional spark plugs as a baseline. With a validated baseline engine simulation, the settings were set for all simulation scenarios at λ=1. Following that, the pre-chambers with and without an auxiliary fuel supply were simulated. In the study of (DI-CNG) SI engine, active TJI was observed to perform better than passive TJI and conventional spark plug ignition. In conclusion, the active pre-chamber with an air channel demonstrated an improved thermal efficiency (η_{th}) over other counterparts and conventional spark ignition systems.

Keywords—Turbulent Jet Ignition, Active Air Control Turbulent Jet Ignition, Pre-chamber ignition system, Active and Passive Pre-chamber, thermal efficiency, methane combustion, internal combustion engine combustion emissions.

S. Ziyaei is with the Department of Mechanical, Manufacturing and Mechatronic Engineering, Royal Melbourne Institute of Technology (RMIT), Melbourne, 3000 Australia and with RMIT University, Australia (e-mail: s3362165@student.rmit.edu.au).

S. K. Mazlan and P. Lappas are with RMIT University, Australia.

I. Introduction and Background

THERE has been a long history of ignition combustion initiation in the pre-chamber of SI engines. It was in fact the 2-stroke Ricardo Dolphin engine that used pre-chamber ignition in 1922 [1]. TJI is primarily used to reduce fuel consumption by achieving complete and stable lean combustion. In contrast, the lean combustion of alternative fuels, such as CNG/Methane with a lower carbon to hydrogen ratio, results in a reduction of emissions. Although lean mixtures are advantageous in internal combustion engines, they have several drawbacks, such as low combustion stability and high misfire rates. This is due to the narrow flammability limit of most fuels used. Misfires and partial burns typically increase the levels of hydrocarbon (HC) and carbon monoxide (CO) emissions due to poor combustion stability. A lean mixture also exhibits a slower flame speed. As is commonly observed, when the lean limit of combustion is exceeded, irregular ignition and HC emissions expand, while power output drastically reduces [2]. Compared to other hydrocarbon fuels, such as propane or gasoline, natural gas requires a higher activation energy. In addition, its flame speed is slower than other fuels, particularly under lean conditions [3], [4].

Therefore, CNG engines require a strong ignition system in order to achieve a stable, complete combustion, especially when operating in lean or stratified conditions. As a solution to lean burn issues, TJI not only provides high energy ignition sources in the combustion chamber, but also enhances combustion by generating extra turbulence. In general, jet ignition systems are divided into Passive (P-TJI) and Active (A-TJI) categories, with the main difference being that an active system has an auxiliary fuel supply within the pre-chamber, illustrated in Fig. 1. Pre-chamber fuel starvation has been alleviated by providing specific fuel supply to the pre-chamber. Passive systems rely on fueling the pre-chamber during the compression stroke via orifices that connect the main chamber and pre-chamber. Passive systems require larger

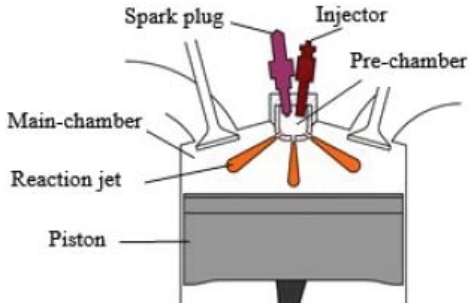

Fig. 1 A schematic illustration of a jet ignition system that includes an additional fuel injector for the pre-chamber [5]

orifices to charge the pre-chamber with air-fuel mixtures. As a result, the velocity of the combusted pre-chamber contents will be reduced as they exit the pre-chamber, resulting in a reduction of penetration rate and turbulence in the main chamber, which ultimately slows down the burning rate.

P-TJI and A-TJI both have the problem of scavenging the pre-chamber from residual gases from the previous combustion cycle. It is more apparent in the case of P-TJI, where the A-TJI achieved partial scavenging success by introducing direct fuel injection into the pre-chamber. Despite the fact that A-TJI helps exhaust residual gases from the cavity, it only partially pushes some gases out of the pre-chamber, not all. These residual gases affect the quality of the mixture inside the pre-chamber, and therefore the quality of the combustion within. In this regard, there is a need for further consideration and possible solutions to the problem.

As shown in Fig. 2, this paper presents a turbulent jet ignition system characterized by an auxiliary Direct Injector (TJI DI) for pre-chamber fueling, as well as an auxiliary air channel connected to a one-way check valve to provide sufficient air to pre-chamber. The prototype design has

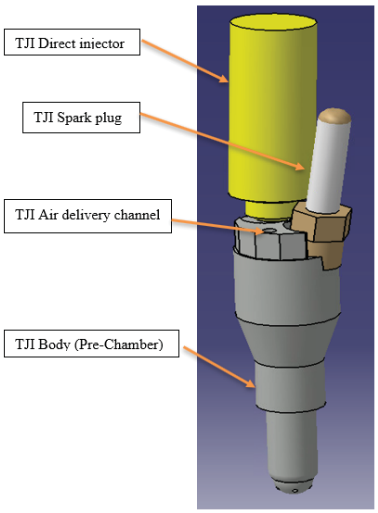

Fig. 2 Computer generated image (CATIA) of the Turbulent Jet Igniter, to be installed onto the cylinder head to replace the spark plug

five small orifices connect the TJI pre-chamber and the main combustion chamber. Due to geometry restrictions, the pre-chamber volume is relatively large, approximately 11.2% of the clearance volume.

The effects of air channels have been discussed throughout this paper. In the pre-chamber, the auxiliary air channel provides sufficient air to create the proper mixture according to the dilution level. The scavenging issue is expected to be resolved by the air provided to pre-chamber via additional air channel. In comparison with conventional spark ignition, the jet ignition system generates a fast burn rate, resulting in successful lean-burn comparable to those obtained with the most efficient internal combustion engine, such as Homogeneous Charge Compression Ignition (HCCI).

The faster burn rates achieved by TJI system allow the compression ratio to be increased when compared to conventional spark ignition configuration [6]. It is also possible to increase the compression ratio when the travel path of the flame front is reduced during flame propagation [7] associated with a distributed jet ignition. This will then reduce the possibility of occurrence of end-gas knock phenomena due to the reduced residence time [8].

A. Study Objectives

By better understanding the combustion process inside the pre-chamber and its effects on the main chamber, it is possible to accurately predict engine performance, optimize the design of the pre-chamber, and improve the combustion efficiency of the engine. A comparison of three pre-chamber ignition systems is carried out at World Wide Mapping Point (WWMP), 1500 (rpm), 3.3 [bar] Indicated Mean Effective Pressure net ($IMEP_{net}$), and 2.6 [bar] Brake Mean Effective Pressure (BMEP). This investigation is based on simulation and has the following specific objectives:

- Compare the pressure rise between conventional ignition configuration and pre-chamber ignition systems.
- Analyze combustion burn parameters and temperature rise rates under stochimetric condition for TJI system and conventional spark ignition system.
- Assess the thermal efficiency produced by a research engine using spark plug, active, passive and air-controlled TJI systems.
- Compare the emission fractions of NO_x, CO_2 and CO in all four ignition configurations.
- Analyze the simulation data to determine if any optimizations are required for the current design based on the data observed.

II. Methodology

As a first step, experimental data were used to validate 3D simulation results. After validating the simulation for the conventional spark plug (baseline), the (P-TJI) 3D results were analyzed and validated. For the validation of these data, cylinder peak pressure, Mass Fraction Burned (MFB), and indicated mean effective pressure (IMEP) are used. AVL Fire simulation settings and codes have been adjusted in accordance with experimental results. The same settings were used to predict combustion parameters such as cylinder peak pressure and MFB to simulate Active TJI. As a next step, a simulation of Active Air Controlled TJI (AAC-TJI) was performed and

the different output data were compared and analyzed. The methodology steps can be seen in Fig. 3.

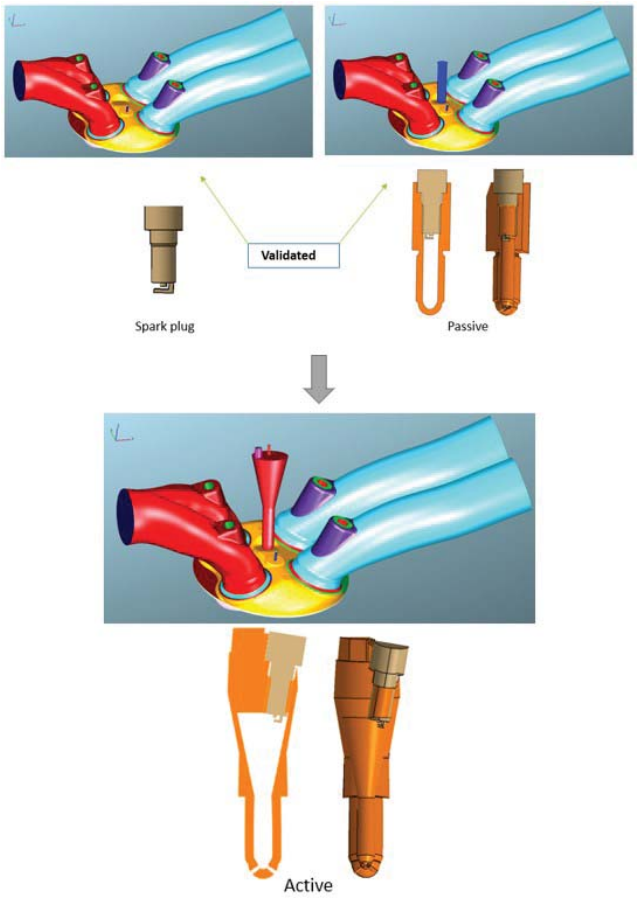

Fig. 3 An overview of the methodology process from the validation of the baseline and passive TJI to the simulation of the active TJI

A 3D simulation of AVL Fire was carried out using experimental data collected at WWMP with the engine speed set to 1500 rpm, $\lambda = 1$ and IMEP=3.3 [bar] for baseline (Spark plug). The CNG was directly injected with a Start Of Injection (SOI) at 569°for a duration of 46°and an ignition timing at 14°before Top Dead Center (bTDC).

Data history records based on crank angels such as intake and exhaust pressure as well as temperature, fuel mass flow data, and lambda number were used as a basis for the CFD program to validate the simulation outputs based on in-cylinder peak pressure, lambda number, IMPE and MFB. Furthermore, passive TJI was also validated in addition to active TJI. A number of these operating conditions obtained from the data acquisition device coupled with dynamometer are illustrated in Fig. 4, which shows the intake and exhaust manifold and in-cylinder pressures as well as ignition and injection timing.

Based on the same boundary conditions, in-cylinder pressure, MFB, in-cylinder temperature, and fraction of $C0$, $C0_2$ and $N0_x$ emissions were investigated when A-TJI and AAC-TJI were used. The engine speed was fixed at 1500 rpm and the intake pressure was maintained in accordance with experimental data in all scenarios. It needs to be noted that the objective of this study is not to determine the lean limit of the directly injected CNG SI engine when the AAC-TJI is employed, but rather to investigate the performance gain that can be achieved by using the AAC-TJI.

TABLE I
SOME OF AVL SINGLE CYLINDER ENGINE SPECIFICATIONS [11]

Engine Parameter	Dimension
Bore	82 mm
Stroke	90 mm
Displacement volume	475.29 cc
Clearance volume	50.03 cc
Con-rod length	147.5 mm
Compression ratio	10.55:1
Intake valve diameter	31 mm
Exhaust valve diameter	27 mm
Valve overlap	18°
Piston crown	2.7 mm deep
Diameter of the Piston bowl (Top)	73 mm
Diameter of the piston bowl (bottom)	63 mm

A. Experimental Research Engine

A single-cylinder AVL research engine was used in the experiments presented in this paper, which is capable of acquiring engine input and output data. The engine is coupled to a dynamometer with a double overhead cam cylinder head. The engine is equipped with a shallow bowl piston crown and a modern pent roof combustion system and has a displacement of 0.4755 liters with a penta [9] cylinder head. Pent roof engines feature double overhead camshafts and four valves per cylinder [10] shown in Fig. 5. An experimental research engine valve lift diagram is shown in Fig. 6. A general overview of the test engine specifications that have been used for Computer Aided Design (CAD) to design a prototype TJI and simulation is presented in Table I. In Fig. 7, some of these features are illustrated in greater detail using the geometric data generated by CATIA for extruding the inner volume of the experimental test engine. This is done in order to simulate all the events required to predict in one cycle in this study.

For partial load engine operating points, a sweep of the start of injection (SOI) is conducted for both early and late injection periods with the objective of determining the optimum SOI in terms of the lowest coefficient of variation (CoV) in IMEP and fuel flow rate. SOI occurs during the valve open period for early injection, and during or after the intake valve closure for late injection. The ignition dwell time is kept constant at 3 miliseconds and the ignition timing is optimized so that 50% of the mass fraction burns is between 8°and 10°after TDC (CA50).

B. Fuel Injection and Ignition Systems

To inject the required fuel mass, a Bosch GDI multi-hole injector is operated by a National Instruments (NI DIDS-2012) injector driver. The fuel pressure is maintained at 100 bar throughout the experiment. By means of two pressure regulators, natural gas is delivered from commercial CNG cylinders to the injector in two stages of pressure reduction (200-150 bar and 150-100 bar). In order to measure the fuel flow rate, a Coriolis flow meter (Siemens Sitrans FC300) is connected to a mass flow reader (Siemens Sitrans). The

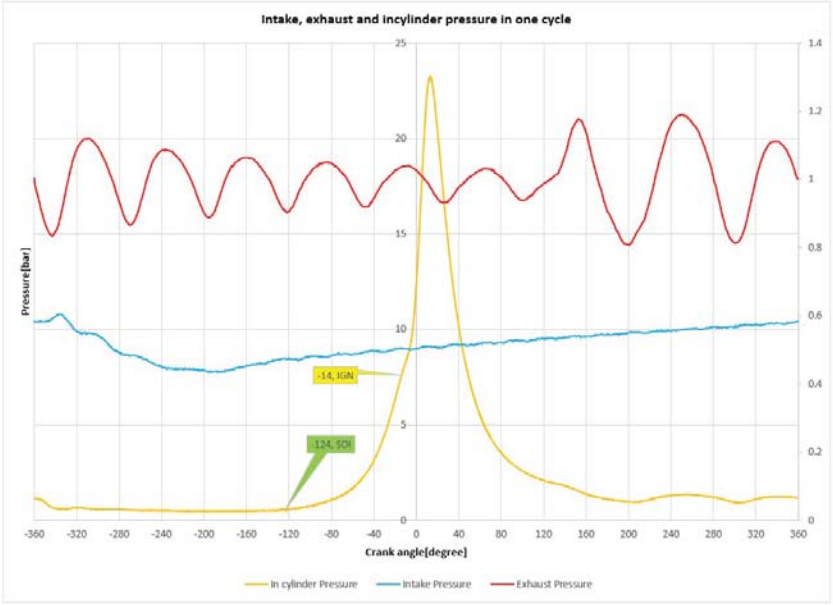

Fig. 4 Test engine data, including in-cylinder, intake and exhaust manifold pressures, for a baseline configuration at WWMP

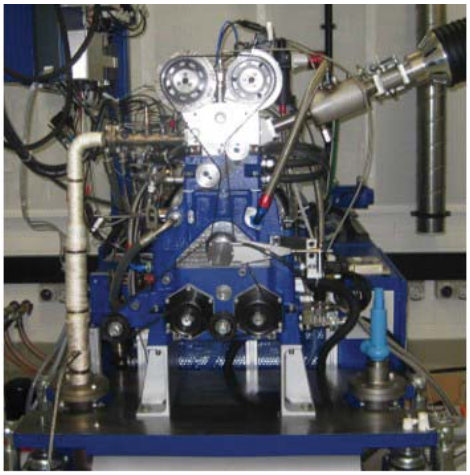

Fig. 5 AVL test engine setup at Green Engine Laboratory (GEL) RMIT University Bundoora, Australia

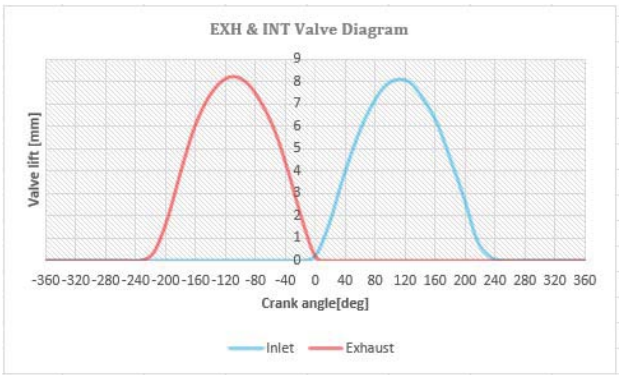

Fig. 6 AVL test engine range of intake and exhaust valve lift events at zero degrees

temperature of the engine oil and coolant is maintained at

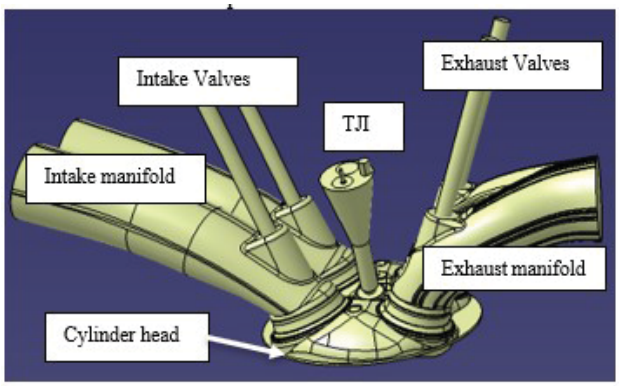

Fig. 7 Test engine interior volume extruded in CATIA for simulation

80°C. There is approximately 90% methane content in the CNG provided to the laboratory, which has an energy content of 44.68 [MJ/kg]. Data collection, including in-cylinder pressure measurement, is conducted for 300 consecutive cycles, and the average values are presented. AVL controllers also transmit Transistor-Transistor Logic (TTL) to the ignition coil, allowing full control of ignition timing and duration.

III. AVL Fire 3D Simulation Validation

Upon completion of multiple test scenarios at WWMP, all data were recorded. These data include intake and exhaust manifold pressure and temperature, as well as lambda readings and fuel mass. For the purposes of comparison, output data such as in-cylinder pressure, Mass Fraction Burned (MFB) and CoV were recorded once the WWMP condition is reached (1500 rpm, partial load, $\lambda = 1$ and IMEP = 3.3 [bar]). Based on the initial and boundary conditions, a full cycle simulation was conducted and the outcome results were compared with experimental data.

An engine cycle was simulated using conventional spark ignition (baseline) based on experimental data. The same final validated setting for simulation of passive TJI (P-TJI) was applied after validating the 2D results against experimental data. Once the 2D results of P-TJI have been validated and all adjustments have been made, these settings and input data will be used to predict the combustion behavior of Active TJI (A-TJI) and Active Air Controlled TJI (AAC-TJI).

WWMP was chosen as the condition for validating baseline and P-TJI due to the availability of experimental data. Data that were validated for these conditions were used to predict the performance gain and loss by the same research engine when all boundary conditions were set in accordance with the experiments. By doing so, the engine speed was maintained at 1500 rpm, the intake manifold pressure was set at the same level as in the experiments. The timing and duration of fuel injection were the same in order to achieve $\lambda = 1$. Under these conditions, it is expected that Mass Fraction Burned (MFB), IMEP, Coefficient of Variation (CoV) and emissions would not differ from experimental data.

As a result of successfully completing simulations for both A-TJI and AAC-TJI, other parameters, such as the cylinder peak pressure, IMEP, and MFB, were compared. Following the review of these data, possible advantages, disadvantages, and optimizations will be discussed.

A. Verification of The Baseline Simulation

In the first stage, the baseline was validated using the data acquired from the test engine. A comparison was made between the in-cylinder pressure trace and the MFB of the combustion simulated by CFD. The simulation and experiment were conducted by direct injection of CNG with SOI @ 90°before TDC for a duration of 46°. Since fuel injection strategy is late, the air/fuel mixture in the main chamber and around spark plug electrodes are considered in-homogeneous. As a result of reading data from a wide band Lambda closed-loop control system (ETAS), λ was maintained at 1 (stoichiometric condition) and ignition timing was set to 14°bTDC.

The maximum peak pressure achieved by simulation is similar to that achieved by experiment, as shown in Fig. 8. However, there is a slight increase in the simulation result that is negligible when compared to the experiment result. This indicates that the simulation model is accurate in predicting the peak pressure due to the similarity of the results. It also suggests that the slight increase in the simulation result is likely due to the numerical approximation of certain parameters in the model.

The MFB was also checked against experimental data in order to verify the accuracy of the combustion simulation results. MFB of the gas mixture in combustion processes as functions of combustion duration reflect the percentage of fuel consumed at each time point. This is an important characteristic of an engine that can be used to assess the performance of the fuel combustion process. The validation of the MFB for the baseline can be seen in Fig. 9.

Comparing the results of MFB, it appears that simulation reached 5% burn slightly faster (1.2%) than experiment. Due to

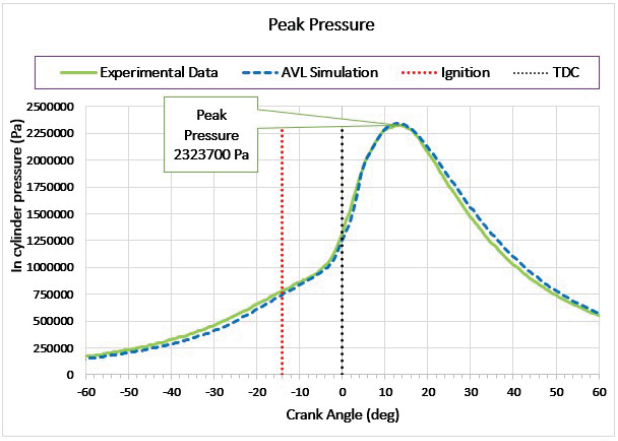

Top Dead Centre (TDC) @ 0 deg CA	
Fuel injection timing (Start of Injection) – degCA	-90°
Ignition timing - degCA	-14°
Engine Speed-RPM	1500
Lambda	1
IMEP-bar	3.3

Fig. 8 Validation of baseline AVL simulation results by comparing the peak in-cylinder pressure with the experimental engine test condition

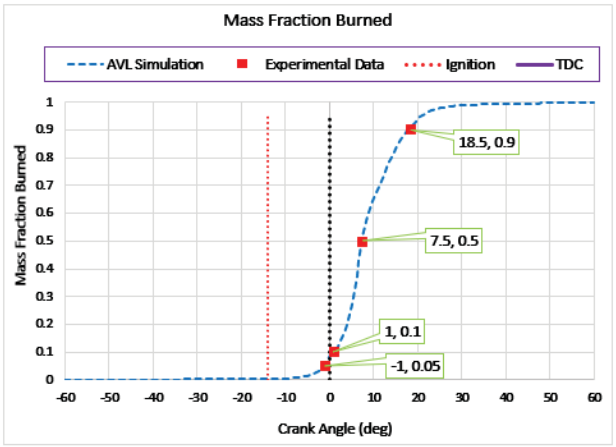

Top Dead Centre (TDC) @ 0 deg CA			
Mass fraction burned	Experiment	Simulation	Error%
5%	-1	-1.012	1.2(Faster)
10%	1	1	0
50%	7.5	7.5	0
90%	18.5	18.5	0
90%~10%	17.5	17.5	0

Fig. 9 Comparison of MFB results with experimental engine data for validation of baseline AVL simulation at WWMP

the fact that the difference between 90% and 10% fuel burn is commonly used to express burn duration, the faster burn at 5% can be ignored. The higher margin in peak pressure obtained by simulation compared to experiment is explained by the faster combustion up to 5% mass fraction burned. According to the graph and table provided, the simulation corresponds closely to the experimental data, and therefore, the baseline simulation is valid. Following the validation of the baseline

setting, the passive TJI simulation needs to be validated, so the accuracy of the CFD can be confirmed for applications involving pre-chamber ignition systems.

B. Verification of the Prototype Passive TJI Simulation

Following the successful verification of AVL Fire simulation results for direct injection CNG SI engines with conventional spark plugs, passive TJI simulation results need to be verified. In order to verify the CFD simulation, a passive pre-chamber (P-TJI) was designed, manufactured, and tested on the same research engine. An illustration of the passive TJI used in the test engine and its orientation when installed on the cylinder head is shown in Fig. 10. As part of the validation

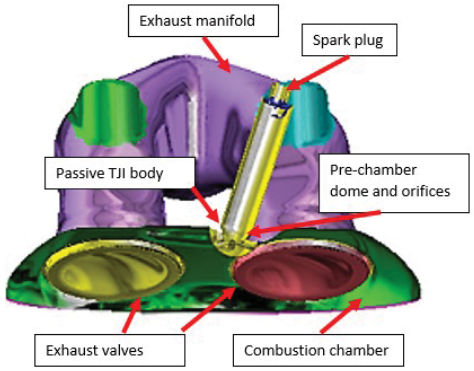

Fig. 10 Pre-processed CAD of P-TJI for the research engine showing the orientation of the pre-chamber on the cylinder head

process, the peak pressure was compared to determine whether the prediction of the simulator was accurate for pre-chamber applications.In order to meet WWMP conditions, experiments were carried out with different conditions for P-TJI. Due to the lack of an auxiliary injector for the pre-chamber, the P-TJI must be fueled by the main chamber mixture through the compression stroke. Therefore, the SOI has been adjusted to 300°bTDC, during which the intake valves are open. As a result, a homogeneous mixture assumed be formed, since there is sufficient time to mix the fuel and air inside the main chamber. Due to the fact that the pre-chamber has a cavity that connects to the cylinder head, the clearance volume will increase, which will cause the compression ratio to be reduced, impacting engine performance and thermal efficiency. A reduction in efficiency is caused by the fact that experimental boundary conditions must be maintained in terms of air/fuel ratio, SOI, ignition timing, and intake pressure and temperature. This is done by maintaining the $\lambda = 1$, instead of finding the lean limit, which results in a reduction in fuel consumption and an improvement in thermal efficiency.

Due to the delay in combustion propagation within the pre-chamber, the ignition timing was also set at 40°bTDC. In a similar manner, the peak pressure predicted by simulation was compared with the experiment and found to have very small variances that could be ignored. This can be seen in Fig. 11.

As it is illustrated in Fig. 12, combustion is slightly slower compared to the experiment. This can be seen more clearly at the beginning up to 5% MFB. From 5% to 10%, a smaller delay results in a 0.37% improvement in burn duration. Until

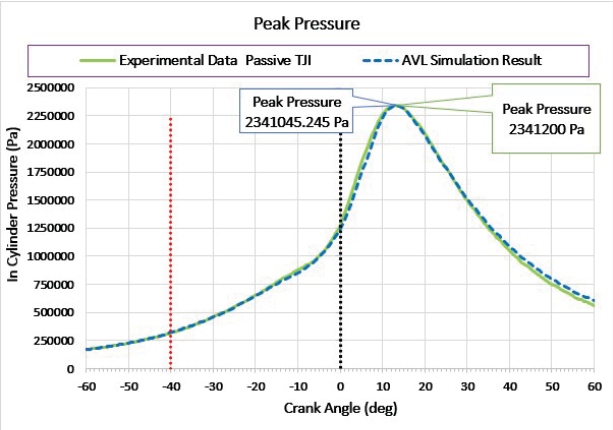

Top Dead Centre (TDC) @ 0 deg CA	
Fuel injection timing (Start of Injection) – degCA	-300°
Ignition timing - degCA	-40°
Engine Speed-RPM	1500
Lambda	1
IMEP-bar	3.3

Fig. 11 Comparison of peak cylinder pressure for passive TJI simulation and experiment at WWMP

50% and then up to 90%, this trend has slowed down a bit. Compared to experiment, the 10-90% MFB was slightly slower in simulation with a 0.51% error margin. This is, in fact, evident in Fig. 11 as a small drop in peak pressure, which is due to a slight delay in combustion. In light of the small variance between simulation and experiment, which is less than 1%, validation was accepted and the setting was used for the A-TJI and AAC-TJI simulations.

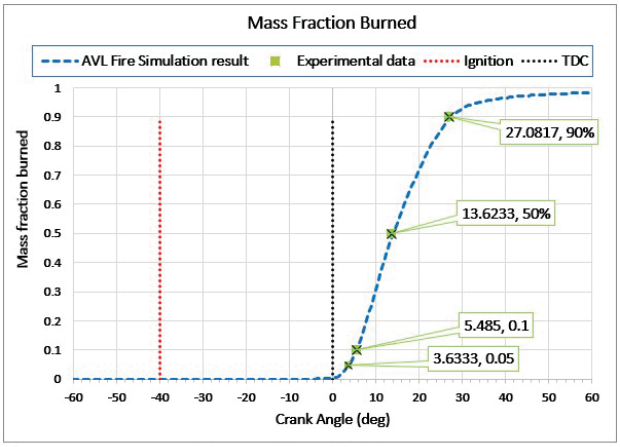

Top Dead Centre (TDC) @ 0 deg CA			
Mass fraction burned	Experiment	Simulation	Error%
5%	3.63	3.65	0.55
10%	5.49	5.5	0.18
50%	13.62	13.66	0.29
90%	27.08	27.20	0.44
90%~10%	21.59	21.7	0.51(Slower)

Fig. 12 Comparison of MFB results with experimental engine data for validation of P-TJI AVL simulation at WWMP

IV. Simulation Results and Discussion

Based on the successful validation of baseline and P-TJI, the same CFD settings were applied for prediction of engine performance with A-TJI and AAC-TJI. As a result, the fuel amount was adjusted to maintain $\lambda = 1$, while maintaining the same intake temperature and pressure as the experiment. An analysis of the discussion section compares the performance of all four ignition system configurations in terms of peak in-cylinder pressure, gain or loss of the IMEP, and, therefore, thermal efficiency. Additionally, the reference cell temperature, the MFB, and the emissions are compared.

The point that needs to be highlighted is that due to the increasing clearance volume and following that the entire domain volume when pre-chamber devices are used, more air will fill up the cylinder, which means a higher quantity of fuel would be needed to attain stoichiometric condition($\lambda = 1$). Therefore, according to (4) [12], the IMEP and, subsequently, the thermal efficiency of the engine would be affected by the volume of the pre-chamber.

$$W_i = \oint P.dV \tag{1}$$

W_i is indicated work per cycle, P is pressure and d_V is volume deference per each crank angle. Therefore, indicated power W_{dot_i} can be expressed as (2):

$$W_{dot_i} = \frac{W_i N}{n_R} \tag{2}$$

where N is crankshaft speed in revolutions per second and n_R is number of crankshaft revolutions per cycle. This is two for four stroke engines and one for two stroke engines. From (2), IMEP can be written as follows with V_d is a displacement volume:

$$IMEP = \frac{W_i}{V_d} \rightarrow IMEP = \frac{(W_{dot_i} n_R)}{V_d N} \tag{3}$$

Therefore, (3) thermal efficiency (η_{th}) can be expressed as a function of the $IMEP$, displacement volume (V_d) over mass of fuel consumed per cycle (m), and calorific value (C_V) of the fuel.

$$\eta_{th} = \frac{IMEP.V_d}{m.C_V} \tag{4}$$

The theoretical thermal efficiency in the Otto cycle is related to γ (specific heat ratio of the working fluid) and r_c (compression ratio) as shown in (5) or (6).

$$\eta_{th} = 1 - \frac{1}{r_c^{(\gamma-1)}} \tag{5}$$

$$\eta_{th} = 1 - \left(\frac{1}{\epsilon}\right)^{k-1} \tag{6}$$

$$k = \frac{C_p}{C_v} \tag{7}$$

In (5), *rc* is compression ratio and γ (gamma) is the specific heat ratio equal to $\frac{C_p}{C_v}$ or $\frac{C_p}{(C_p - Rgas)}$. Equation (5) can be written in form of (6), where ϵ is the compression ratio or the expansion ratio, C_v and C_p are the specific heat at constant volume and pressure. According to this theory, increasing the engine compression ratio and the specific heat ratio are effective ways for improving thermal efficiency[13]. In other words, (5) explains higher thermal efficacy achievement by raising the mechanical compression ratio and extending the lean burn or by optimizing the opening timing of the exhaust and intake valves. Equation (7) shows how lean burn combustion can result in higher thermal efficiency [13]. There is a negative effect as a result of increasing the clearance volume, which affects the compression ratio. Accordingly, slight shortcomings are apparent in the performance achieved by P-TJI, as well as possibly A-TJI.

A. In-cylinder Pressure Trace Comparison

To compare all four scenarios, validated settings were used as well as boundary conditions for all simulations. Because of poor performance of the prototype P-TJI, it was redesigned and tested in the engine to achieve the most optimal results by reducing ignition advance. Optimized P-TJI has a smaller cavity volume and spark plug electrodes are located closer to the main chamber than the prototype one. Table II lists some of these simulation conditions. As we can see, SOI is at 151°bTDC for a duration of 46°, ignition timing (IGN) is at 14°bTDC, engine speed is kept constant at 1500 rpm, and lambda is 1. The SOI for the fuel injector in the A-TJI and the AAC-TJI is set at 20°bTDC with a duration of 5 degrees bTDC. There are two sequences of injection on the AAC-TJI air injector, with the first starting at 135°after TDC and continuing for 15°. The second sequence begins at 35°bTDC and ends right before pre-chamber fueling occurs.

It is important to note, however, that only the first sequence of air injection was simulated and discussed in this paper. Further simulations are necessary to fully understand the implications of injecting different amounts of air into the combustion chamber. Therefore, only the scavenging improvement of the AAC-TJI has been achieved and demonstrated using AVL Fire simulation. The impact of adding pre-chamber devices, P-TJI, A-TJI, and AAC-TJI is also highlighted in the same table as the reduction in compression ratio. Based on (5), this reduction will have a negative impact on thermal efficiency, which will offset the thermal efficiency improvements achieved by TJI.

Fig. 13 illustrates the in-cylinder pressure trace for each of the four scenarios. In pre-chamber configurations, peak pressure would not be optimal without sweeping the ignition timing. In P-TJI configuration, this is more pronounced, even though the type II pre-chamber device, with its smaller cavity and modified spark plug location, could not achieve a better peak pressure than baseline. Pressure trace for P-TJI indicates a delay in pressure rise due to the time required for hot combustion gases to exit the pre-chamber orifices. One of the main reasons for this is the lack of an auxiliary fuel injector in the pre-chamber, as well as residual gases from the previous combustion cycle, affecting the quality of the mixture. As a result of using the more suitable mixture inside the pre-chamber, combustion will be improved, resulting in an increased pressure rise within the pre-chamber, thereby reducing this delay. As a result of increasing the ignition

TABLE II
SIMULATION BOUNDARY CONDITIONS FOR SPARK PLUG, P-TJI, A-TJI, AND AAC-TJI IGNITION CONFIGURATIONS

Boundary condition	Baseline	P-TJI	A-TJI	AAC-TJI
Start of injection (SOI)	-151°	-151°	-151°	-151°
Injection duration(DOI)	46°	46°	46°	46°
Pre-chamber SOI	NIL	NIL	-20°	-20°
Pre-chamber DOI	NIL	NIL	5°	5°
Ignition timing	-14°	-14°	-14°	-14°
Displacement volume(V_d)[cc]	475.29	475.29	475.29	475.29
Clearance volume(V_c)[cc]	50.03	51.86	54.53	55.23
Compression ratio(C_R)	10.55:1	10.16:1	9.72:1	9.61:1
C_R reduction	0	3.65%	7.86%	8.91%
air/fuel ratio (λ)	1	1	1	1

advance timing, this delay will be reduced, not only because the process of reaction chain progress will occur earlier, but also because less compression inside the P-TJI cavity will result in faster combustion propagation. As a result, hot, high-energy gases will exit the pre-chamber earlier, igniting the mixture in the main chamber sooner and increasing the peak pressure in the cylinder.

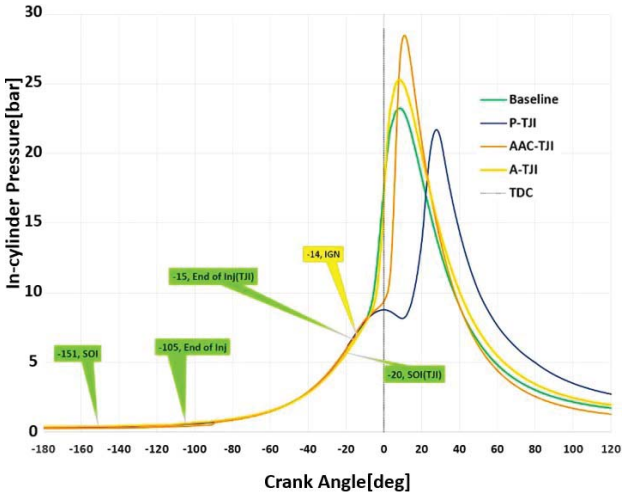

Fig. 13 Simulation pressure trace comparison for spark plug, P-TJI, A-TJI, and AAC-TJI ignition configurations at 1500 rpm, part load, and $\lambda = 1$

Conversely, the A-TJI configuration shows a higher peak pressure than the baseline and P-TJI configurations. Clearly, this is due to the use of an additional direct fuel injector. Furthermore, direct injection of fuel at high pressure ($100[bar]$) within a short period of time ($555\mu S$) could result in residual gases from the previous combustion cycle exiting the cavity right before ignition and entering the main chamber. Therefore, there is a reduction in the dilution of the pre-chamber mixture. The residual gases will enter the main chamber, which is not an ideal situation. Improved scavenging and a richer mixture inside the pre-chamber will result in much faster and hotter combustion when compared to P-TJI.

A rich mixture ($\lambda = 0.85$) inside the pre-chamber of A-TJI makes the propagation of the flame kernel much faster than P-TJI, which results in a shorter delay in combusting the main chamber mixture. AAC-TJI has a slightly leaner pre-chamber mixture ($\lambda = 0.95$) than A-TJI, which causes an initial delay in pressure rise. Since A-TJI's pre-chamber mixture contains impurities, the AAC-TJI pre-chamber mixture has a more complete combustion. Thus, the pressure inside the cavity will increase. This will result in an increase in the speed of the hot jet gases emerging from the orifices and entering the main chamber with high turbulence energy. It is the turbulence created by AAC-TJI that has made a significant difference in terms of the peak pressure achieved. This can be observed by comparing the maximum Mean Turbulence Kinetic Energy (MTKE) in each scenario. Table III shows that AAC-TJI has the highest turbulence kinetic energy followed by A-TJI and P-TJI. This has affected the rate of heat release and, consequently, the peak pressure for AAC-TJI.

TABLE III
SIMULATION RESULTS OF MEAN TURBULENCE KINETIC ENERGY (MTKE) FOR SPARK PLUG, P-TJI, A-TJI, AND AAC-TJI IGNITION CONFIGURATIONS

Ignition device	Baseline	P-TJI	A-TJI	AAC-TJI
MTKE befor ignition [$\frac{m^2}{s^2}$]	11.15	11.99	11.85	12.09
MTKE @ TDC[$\frac{m^2}{s^2}$]	12.18	15.58	23.84	29.02
Maximum MTKE[$\frac{m^2}{s^2}$]	38.24	41.54	43.96	48.45
MTKE variation %	0	8.61	14.94	26.69

Due to injection of air for 15°starting at 135°bTDC during exhaust stroke, right before the closure of the exhaust valves, residual gases will be directed out of the pre-chamber and then out of the main chamber. As a result, when the intake valve opens, pure air enters the main domain during the intake stroke as well as the pre-chamber during the compression stroke.

B. Mass Fraction Burned Results and Comparison

In the validation section, MFB was discussed as one of the main combustion characteristics of internal combustion engines which tends to define the behavior of the combustion regime. It is important to note that MFB plays a major role in the overall combustion performance of an engine, affecting the combustion rate and fuel consumption. However, it is also worth mentioning that MFB is not the only combustion characteristic that affects the combustion rate and fuel consumption of an engine. There are other factors, such as the air-fuel mixture, the compression ratio, and the ignition timing, that also play a role in the overall combustion performance of an engine.

Based on the MFB data extracted from the AVL Fire simulation, Fig. 14 illustrates that AAC-TJI has the fastest burning rate. In comparison to baseline and P-TJI, A-TJI also had a faster burn rate and a shorter burn duration. There was a marginal difference between A-TJI and AAC-TJI before 5% and after 90% MFB. Table IV provides the MFB and burn duration for each simulation scenario.

According to the analysis of the P-TJI MFB diagram, the ignition configuration revealed that despite a slower burn rate

TABLE IV
SIMULATION RESULTS MFB COMPARISON FOR SPARK PLUG, P-TJI, A-TJI, AND AAC-TJI IGNITION CONFIGURATIONS

Mass Fraction Burned	Baseline	P-TJI	A-TJI	AAC-TJI
MFB(5)%	-1.2°	1°	-3.5°	-6°
MFB(10)%	1°	3°	-1°	-2°
MFB(50)%	7.5°	8.5°	5°	3°
MFB(90)%	18°	21°	16°	14°
MFB(10-90)%	17°	18°	17°	16°
Burn duration	Ref	Longer	Ref	Shorter

from 5% to 50% MFB, when hot jets are expelled through the orifices, the burn rate increases to match the burn rate at 90% MFB. In comparing the results in Table IV with Fig. 13, it is apparent that burn duration and pressure rise are directly related. Among all ignition configurations, AAC-TJI has shown rapid combustion specifically between 5% and 50% and an overall angular shorter burn of 5.9%. Furthermore, the generated pressure after ignition was much higher for AAC-TJI compared to other configurations, indicating a more efficient combustion process.

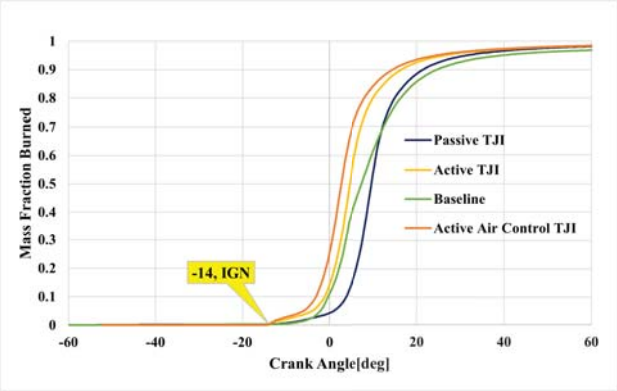

Fig. 14 Comparison of fuel mass fraction burned simulation for spark plug, P-TJI, A-TJI, and AAC-TJI ignition configurations at 1500 rpm, part load, and $\lambda = 1$

C. Temperature Comparison at the Reference Cell

A temperature measurement has been made at the reference cell this time. Since the fuel amounts have been adjusted so that $\lambda = 1$ is achieved, the configuration with the higher peak pressure appears to be the one with the higher in-cylinder temperature. The temperature curves for each scenario at the reference cell are illustrated in Fig. 15. As a result of the fast and turbulent combustion of the AAC-TJI, the temperature rise rate and mean temperature have been the highest among the other configurations.

It is also found that the A-TJI configuration exhibits the fastest temperature rise rate and the second highest temperature at the reference cell. While the P-TJI showed a slightly lower peak pressure, it demonstrated a higher temperature growth rate but a slightly lower peak temperature as a result of the rapid burning mechanism of the pre-chamber device. As a result, hot jets seeded within the main chamber will initiate a rapid segmentation reaction throughout the mixture within the main chamber.

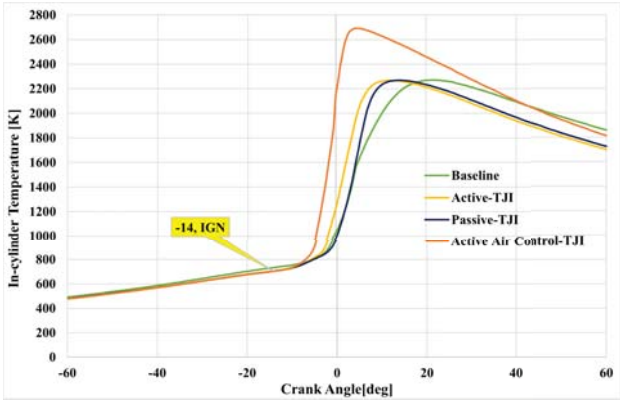

Fig. 15 In-cylinder temperature simulation result comparison for spark plug, P-TJI, A-TJI, and AAC-TJI ignition configurations at 1500 rpm, part load, and $\lambda = 1$ at reference cell

Due to the stable and complete combustion in AAC-TJI, it was determined that the temperature increase rate was the fastest among the rest of the pre-chamber devices, supporting the idea of having air injection to scavenge the pre-chamber to produce improved pre-chamber combustion, resulting in faster burn in the main chamber. Table V shows the simulation mean temperature results of all ignition devices as compared to one another.

TABLE V
SIMULATION RESULTS OF MEAN TURBULENCE KINETIC ENERGY (MTKE) FOR SPARK PLUG, P-TJI, A-TJI, AND AAC-TJI IGNITION CONFIGURATIONS

Ignition device	Baseline	P-TJI	A-TJI	AAC-TJI
Maximum Temperature [K]	2230	2268	2285	2692
Max Temp @ CA [deg]	21.5°	13.5°	12°	4.5°
Max Temp to IGN [deg]	35.5°	27.5°	26°	18.5°
Max Temp growth %	Ref	Higher by 1.7%	Higher by 2.5%	Higher by 20%
Max Temp time duration %	Ref	Shorter by 22.5%	Shorter by 26.7%	Shorter by 47.8%

According to the analysis of the cylinder pressure diagram Figs. 13 and 14, it is evident that to produce higher IMEP and thereafter, higher thermal efficiency, rapid heat release in other words, a very fast burn, is not the only effective factor. The P-TJI, with the higher heat release and maximum temperature in comparison to baseline, has achieved a lower IMEP than baseline as we discussed earlier. The reason for that is to compare all four scenarios at the same ignition timing as the optimal baseline ignition timing is at 14°bTDC. Therefore, after advancing the ignition timing more than 14°bTDC at WWMP condition, the IMEP achieved by baseline configuration will actually decrease. For this reason, the same ignition timing was used for all scenarios, which resulted in a slight decline for P-TJI, a small gain for A-TJI, and the best results for AAC-TJI. In addition, Table VI provides a more detailed analysis of this comparison.

TABLE VI
IMEP AND HEAT RELEASE RATE COMPARISON FOR SPARK PLUG, P-TJI, A-TJI, AND AAC-TJI IGNITION CONFIGURATIONS

Ignition device	Baseline	P-TJI	A-TJI	AAC-TJI
IMEP acheived [bar]	3.3	3.05	3.46	3.85
IMEP comparison	Ref	-7.5%	4.9%	16.7%
Heat release comparison	Ref	1.7%	2.5%	20%

D. Comparing Simulation Emission Results

AVL Fire uses computational fluid dynamics (CFD) to calculate the concentrations of species and fractions in the combustion domain. It takes into account the effects of turbulence, chemical reactions, and heat transfer, as well as the initial conditions of the fuel, oxidizer, and air. For instance, the software can accurately estimate the temperatures and pressures of the reaction zone. It can also estimate the concentrations of the main species, such as carbon dioxide, carbon monoxide, nitrogen, oxygen, and water vapor. Based on the emission model of the AVL, simulation results for all four scenarios were in line with the results of previous sections regarding pressure and temperature. Table VII shows the simulation emission comparison between all ignition configurations.

TABLE VII
SIMULATION EMISSION FRACTION COMPARISON FOR SPARK PLUG, P-TJI, A-TJI, AND AAC-TJI IGNITION CONFIGURATIONS

Ignition device	Baseline	P-TJI	A-TJI	AAC-TJI
NO_x fraction	2.0E-3	1.0E-3	2.0E-3	5.0E-3
CO_2 fraction	1.6E-1	1.7E-1	1.4E-1	1.1E-1
CO fraction	1.3E-1	1.2E-1	1.1E-1	1.0E-1

According to Chaichan and Abass [14], NO_x formed by the stabilization of atmospheric nitrogen in oxidizing atmospheres at high flame temperatures exceeding 1573 K or 1300 °C. There is a general production of thermal NO_x during the combustion of either gases or fuel oils. When combustion takes place under fuel-lean conditions (with less air) and the temperature rises, there will be an increase in NO_x emissions due to the formation of oxygen radicals. As opposed to this, the oxidation reaction will involve the OH and H radicals when combustion occurs in fuel-rich conditions [15]. As a result, it is evident that AAC-TJI exhibits the highest NO_x fraction based on the higher pressure and temperature compared to the rest of the ignition devices, with A-TJI ranking second in terms of NO_x emission fraction when comparing Figs. 13 and 14, and Table VII. In contrast to the rest of the pre-chamber devices and baseline, P-TJI emits significantly less NO_x because of a colder combustion and smaller peak pressure. As a result of complete combustion, A-TJI and AAC-TJI showed the lowest levels of CO_2 and CO emissions, while P-TJI showed the greatest levels of CO_2 as a result of slow, unstable combustion. The cooler combustion of P-TJI helps reduce the production of NO_x, but the slower, less stable combustion produces more CO_2. A-TJI and AAC-TJI have the advantage of higher combustion temperatures and better stability, which leads to complete combustion of the fuel and fewer pollutants except NO_x. The emissions of nitrogen oxide can be reduced by the use of a leaner mixture after reaching a certain level and by the use of some exhaust after treatment.

V. CONCLUSION

For decades, engine manufacturers have sought ways to reduce fuel consumption and increase efficiency including though methods such as stratified charge combustion and lean burn. High energy ignition systems are needed for ultra-lean and stratified charge combustion. An example of a high energy ignition device is Turbulent Jet Ignition (TJI). A pre-chamber ignition system generates distributed ignition sources by using hot turbulent jets of combustion gases. Even in high burning dilute mixtures and or slow burning fuels like CNG, the distributed ignition sites result in relatively short flame travel distances and short combustion duration. This will result in major improvements in peak thermal efficiency at part load of engines with pre-chamber ignition system.

Through the CFD simulation, important outcomes were achieved. Furthermore, these results laid the foundation for further testing and optimization. Some of these outcomes are as follows:

- AAC-TJI achieved higher peak pressures than baseline, A-TJI, and P-TJI at the same $\lambda = 1$.
- AAC-TJI produced more heat at $\lambda = 1$ due to its fast complete combustion.
- AAC-TJI provides the shortest burn compared to A-TJI, P-TJI and baseline.
- AAC-TJI used a leaner fuel mixture than A-TJI, but turbulence inside the main chamber caused more rapid burning, resulting in higher peak pressure.
- With pre-chamber ignition devices, depending on the type of the device, Passive or Active, ignition timing needs to be advanced compared to baseline.
- When AAC-TJI is used, the temperature and pressure rise, causing higher NO_x amounts which must be treated by exhaust, or with a leaner mixture.
- Thermal efficiency will be adversely affected by pre-chamber devices due to increased clearance volume, which will decrease the compression ratio. Peak pressure improvement and lean burn will overcome the negative effects.

The simulation resulted in a more accurate model of the system behavior and allowed for better predictions of the effects of changes in the system. Additionally, it allowed for the optimization of the system and the identification of potential areas of improvement. These areas of the investigation to achieve optimum results by using AVL Fire 3D simulation CFD are as follows:

- Study the optimum ignition timing based on the fuel and air injection events at part load condition.
- Examine the negative effects of reducing the compression ratio by adding the cavity volume to the clearance volume, and then apply multiple air injection sequences to minimize the reduction by using AAC-TJI.
- Analyze the heat loss through the AAC-TJI and the effects on combustion; in addition, investigate the addition coating inside the pre-chamber cavity to change

the thermal conductivity (K) of the AAC-TJI to gain improvements.
- Compare the combustion performance of different AAC-TJI designs with the smaller volume and surface area of the pre-chamber.
- Analyze comprehensively the AAC-TJI orifices in terms of size, length, and angle, and their effects on combustion.
- By using the AVL Fire CDF, find the optimal design and examine the maximum efficiency and emission reduction achieved by AAC-TJI.

A comprehensive analysis must be conducted to determine the optimal design features that will maximize the benefits of an Active Air controlled TJI. Utilizing greener fuels, such as compressed natural gas, will help to achieve the main objective of the novel TJI, which is to improve thermal efficiency and reduce emissions.

ACKNOWLEDGMENT

The authors would like to thank RMIT University for the opportunity to conduct the research and AVL for the software and licenses provided.

REFERENCES

[1] M. C. Turkish, "*3-valve Stratified Charge Engines: Evolvement, Analysis and Progression*", SAE Transactions, vol. 83, 1974, pp. 3483–503. JSTOR. [online].Accessed: Dec. 08, 2022. Available: http://www.jstor.org/stable/44723973.

[2] E. Toulson et al., "*Visualization of Propane and Natural Gas Spark Ignition and Turbulent Jet Ignition Combustion*", SAE International Journal of Engines, vol. 5, no. 4, pp.1821-1835, 2012, doi: https://doi.org/10.4271/2012-32-0002.

[3] A. De, D. S. K. Ting, and M. D. Checkel, "*The Effects of Temperature and Pressure on Stretched, Freely Propagating, Premixed, Laminar Methane-Air Flame*, SAE Technical Paper Series. SAE International, 2006, doi: 10.4271/2006-01-0494.

[4] R. Amirante, E. Distaso, P. Tamburrano, and R. D. Reitz, "*Laminar flame speed correlations for methane, ethane, propane and their mixtures, and natural gas and gasoline for spark-ignition engine simulations*," Int. J. Engine Res., vol. 18, no. 9, pp. 951–970, Nov. 2017, doi: 10.1177/1468087417720018.

[5] W. P. Attard, N. Fraser, P. Parsons, and E. Toulson, "*A Turbulent Jet Ignition Pre-Chamber Combustion System for Large Fuel Economy Improvements in a Modern Vehicle Powertrain*," SAE Int. J. Engines, vol. 3, no. 2, pp. 20–37, 2010, doi: 10.4271/2010-01-1457.

[6] S. Couet, P. Higelin, and B. Moreau, "*APIR: A New Firing Concept for the Internal Combustion Engines - sensitivity to knock and in-cylinder aerodynamics*," SAE Tech. Pap., 2001, doi: 10.4271/2001-01-1954.

[7] D. K. Park, H. S. Kim, and W. T. Kim, "*Study of Flame Propagation for Different Combustion Chamber Configurations in an SI Engine*," SAE Technical Paper Series. SAE International, 1997, doi: 10.4271/970876.

[8] W. P. Attard, H. Blaxill, E. K. Anderson, and P. Litke, "*Knock Limit Extension with a Gasoline Fueled Pre-Chamber Jet Igniter in a Modern Vehicle Powertrain*," SAE Int. J. Engines, vol. 5, no. 3, pp. 1201–1215, 2012, doi: 10.4271/2012-01-1143.

[9] T. Kuo and R. D. Reitz, "*Computation of Premixed-Charge Combustion in Pancake and Pent-Roof Engines*," SAE Technical Paper Series. SAE International, 1989, doi: 10.4271/890670.

[10] O. Hadded and I. Denbratt, "*Turbulence Characteristics of Tumbling Air Motion in Four-Valve S.I. Engines and their Correlation with Combustion Parameters*," Feb. 1991, doi: 10.4271/910478.

[11] D. Sankesh, J. Edsell, S. Mazlan, and P. Lappas, "*Comparative study between early and late injection in a natural-gas fuelled spark-ignited direct-injection engine*," Energy Procedia, vol. 110, pp. 275–280, 2017, doi:10.1016/j.egypro.2017.03.139

[12] J. Heywood, "*Internal combustion engine fundamentals*", 2nd Edition, Vol. 2.12, McGraw-Hill, 2018, doi:1260116107. Available: https://www.accessengineeringlibrary.com/content/book/9781260116106

[13] D. Takahashi, K. Nakata, Y. Yoshihara, and T. Omura, "*Combustion Development to Realize High Thermal Efficiency Engines*," SAE Int. J. Engines, vol. 9, no. 3, pp. 1486–1493, 2016, doi: https://doi.org/10.4271/2016-01-0693.

[14] Q. A. Abass and M. T. Chaichan, "*Study of NOx Emissions of S.I. Engine Fueled with Different Kinds of Hydrocarbon Fuels and Hydrogen*," Al-Khwarizmi Eng. J., vol. 6, no. 2, 2010, Accessed: Mar. 08, 2022. [Online]. Available: https://www.iasj.net/iasj/article/2293.

[15] S. Goto, T. Fukuda, and Y. Ono, "*Study on NOx Formation and Reduction of Lean-Burn Spark-Ignited Gas Engine with Pre-Combustion Chamber*," Trans. JAPAN Soc. Mech. Eng. Ser. B, vol. 64, no. 623, pp. 2332–2339, 1998, doi: 10.1299/kikaib.64.2332.

Siyamak Ziyaei received a bachelor's degree in civil and structural engineering in 2004, and a master's degree in international automotive engineering from RMIT University, Australia in 2016. He is currently completing his Ph.D. in Manufacturing and Mechatronic Engineering at RMIT University, Australia with a focus on the ignition system of internal combustion engines. Throughout his career, he has worked primarily in the automotive industry in the areas of vehicle structures, calibration, and powertrains. Currently, he holds a professional membership with Engineers Australia. Among his research interests are:

- Internal Combustion Engines
- Thermal efficiency optimization
- Vehicle structure design and NVH
- Alternative Fuels, less carbon or carbon free

Siti Khalijah Mazlan received her bachelor's degree in 2012, and her Ph.D. in 2017 from RMIT University, Australia. She has worked in the automotive industry primarily in vehicle structures. She is a member of Engineers Australia. Her research interests include:

- Internal Combustion Engines
- Alternative Fuels
- Fuel Injection Strategies

Petros Lappas has a Ph.D. degree in Mechanical Engineering from the University of British Columbia, Canada. Since completing his Ph.D. in 2003 he has worked as a Research Scientist at NRCan in Ottawa, Canada and as a post-doctoral researcher at the High Temperature Gas Dynamics Laboratory at Stanford University, U.S.A. A key component of his research experience is the measurement of quantities such as flow velocity, temperature and chemical

composition using optical systems. His research interests include:

- Improving thermal efficiency of internal combustion engines
- Laser diagnostics of flow and combustion (e.g., PIV, LDV, spectroscopy, flow visualization, CARS) AAC-TJI.
- Aerosols and two-phase flow
- Solar fuels